Collision-broadened spectral line profiles in the limit of high perturber density

N. F. Allard
Département Atomes et Molécules en Astrophysique, Observatoire de Paris–Meudon, 92195 Meudon, France

Y. G. Biraud
Laboratoire d'Astronomie Infrarouge, Observatoire de Paris–Meudon, 92195 Meudon, France

A. Chevillot
Département d'Astrophysique Extragalactique et de Cosmologie, Observatoire de Paris–Meudon, 92195 Meudon, France
(Received 17 February 1987; revised manuscript received 28 September 1987)

In the present research we have used a Fourier spectral analysis to study line profiles due to strong atom-atom interactions in the limit of high perturber density. The presence of multiple satellites in this case is well explained. Moreover, for decreasing interactions and densities we may extrapolate our results and explain the disappearance of the satellites. The use of "a crude potential shape"—here a square-well—proves to be sufficient to explain the presence of multiple satellites and determine the necessary physical conditions for their appearance.

I. INTRODUCTION

Our previous analyses[1–4] of spectral lines of neutral atoms perturbed by collisions lead us to study the limit of very high perturber densities and strong interactions. In this situation the emitted wave trains are always perturbed. The radiator is continuously subject to collisions and the duration of any unperturbed wave trains tends to zero.

For large densities and strong atom-atom interactions, the autocorrelation function exhibits very distinctive features which lead us first to build a model and then to check its mathematical validity. A spectral analysis is then sufficient to explain the existence of the multiple satellites appearing so often in experimental profiles. For decreasing densities and interactions, we also have found the physical conditions necessary for their existence. This is a powerful approach.

This study has allowed us to deduce mathematically a peculiar value of the phase shift induced by the collision which defines a transition between two very different families of profiles. This transition has been observed experimentally[5,6] and previously studied,[2,3] but the analysis presented here provides a new systematic explanation of the phenomenon.

II. THEORY

The spectral line $I(\Delta\omega)$ is the Fourier transform (FT) of the Hermitian autocorrelation function $\Phi(s)$,

$$I(\Delta\omega)=\frac{1}{2\pi}\int_{-\infty}^{+\infty} e^{i\Delta\omega s}\Phi(s)ds \ . \tag{1}$$

$\Phi(s)$ is calculated in the unified Anderson-Talman[7] theory with the assumptions that the radiator is stationary in space, the perturbers are mutually independent, and in our adiabatic approach, that the potentials are scalarly additive.

$\Phi(s)$ is expressed by

$$\Phi(s)=\exp\{-[w(s)+id(s)]\} \ , \tag{2}$$

where

$$w(s)+id(s)=n\bar{v}\int_0^{+\infty} d\rho\, 2\pi\rho \int_{-\infty}^{+\infty} dt(1-e^{i\eta(\rho,t,s)}) \ , \tag{3}$$

n is the perturber density, ρ the impact parameter, and $\eta(t,s)$ the phase shift calculated along a classical path from

$$\eta(t,s)=\int_t^{t+s} V(t')dt' \ .$$

V represents the difference between the energy levels of the transition in units of rad/sec. The interaction potential used here is a square well where $V(R)=V$ for $R<a$, $V(R)=0$ for $R>a$, and R is the internuclear distance.

We assume rectilinear trajectories for the perturbers of uniform velocity $\bar{v}$ $[\bar{v}=(8kT/\pi m)^{1/2}]$. The autocorrelation function is completely analytical and we only need to compute its Fourier transform to obtain the spectral line shape. $\Phi(s)$ depends only on the dimensionless parameters

$$u=\bar{v}s/2a=s/\tau_{\max} \ ,$$

where $\tau_{\max}=2a/\bar{v}$ is the collision time, x, the maximum value of the phase shift,

$$x=2aV/\bar{v}=V\tau_{\max} \ ;$$

and h, the number of perturbers in the interaction volume,

$$h=\tfrac{4}{3}\pi a^3 n \ .$$

There are two different expressions for $\Phi(s)$ depending on whether the value s is less or greater than $\tau_{\max}$.

For $u<1$ we obtain

$$w_1(u)=h\left\{1-\cos(xu)+3\left[u\left[\frac{1}{x^2}+\frac{1}{2}\right]+u\cos(xu)\left[\frac{1}{2}+\frac{3}{x^2}-\frac{u^2}{6}\right]+\frac{\sin(xu)}{x}\left[u^2-1-\frac{4}{x^2}\right]\right]\right\}, \quad (4)$$

$$d_1(u)=h\left\{-\frac{3}{x}\left[1+\frac{4}{x^2}\right]-\sin(xu)+3\left[u\sin(xu)\left[\frac{1}{2}-\frac{u^2}{6}+\frac{3}{x^2}\right]+\frac{\cos(xu)}{x}\left[1+\frac{4}{x^2}-u^2\right]\right]\right\}. \quad (5)$$

For $u>1$ we obtain

$$w_2(u)=\frac{3}{2}hu\left[1+\frac{2}{x^2}(1-\cos x-x\sin x)\right]+h\left\{1+\frac{12}{x^3}\left[x\cos x+\sin x\left[\frac{x^2}{4}-1\right]\right]\right\}, \quad (6)$$

$$d_2(u)=3h\frac{u}{x^2}(x\cos x-\sin x)-\frac{12h}{x}\left\{\frac{1}{4}+\frac{1}{x^2}\left[1+\cos x\left[\frac{x^2}{4}-1\right]-x\sin x\right]\right\}. \quad (7)$$

III. STUDY OF THE AUTOCORRELATION FUNCTION

The autocorrelation function $\Phi(s)$ is composed of several distinct patterns which are seen in Figs. 1(a) and 1(b). This strange shape is rather astonishing at the first sight, but it is easy to model mathematically. The appearance of the satellites is governed by the dependence of the autocorrelation function on the parameters h and x.

An examination of Figs. 1(a) and 1(b) points to three main characteristics. The first striking phenomenon is that $\Phi(s)$ is composed of separate patterns with rather similar appearance. The second is that the patterns are separated by the same time, $s=2\pi/V$. The third is that the maxima of the patterns decrease regularly with increasing s. These three features permit an obvious representation for the correlation function.

Let us denote the pattern centered at $s=0$ by $p(s)$. The quasiperiodic shape of $\Phi(s)$ can be expressed by the convolution of $p(s)$ with Dirac impulses centered at multiples of $2\pi/V$. Hence, a first expression for $\Phi(s)$ is

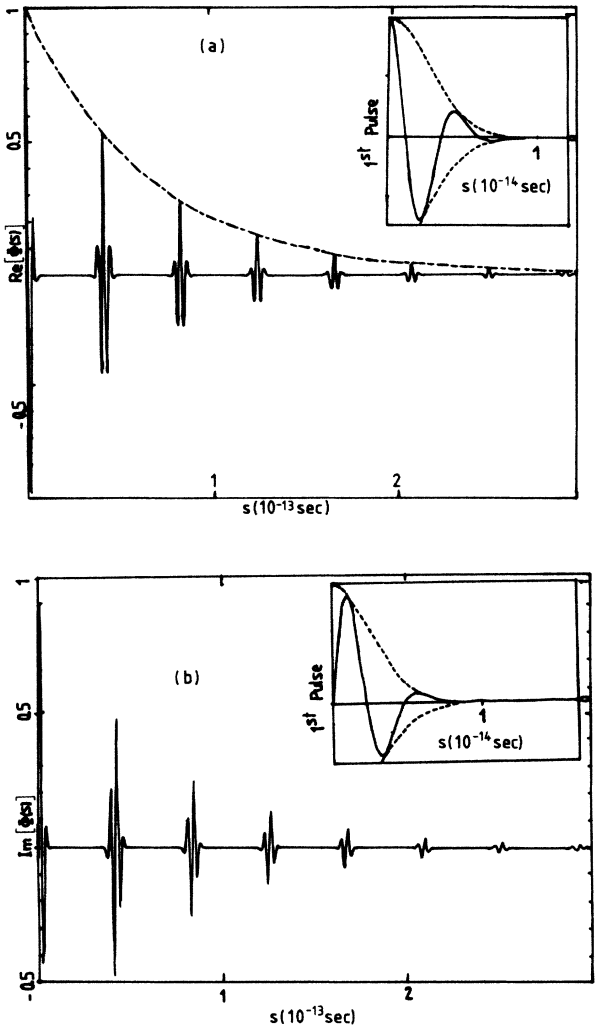

FIG. 1. (a) ——, $\mathrm{Re}[\Phi(s)]$, real part of the radiation autocorrelation function; – – –, the damping function $\gamma(s)$. In the inset: ——, the first even pulse $p(s)$ of $\mathrm{Re}[\Phi(s)]$ represented for $s\geq 0$; — — —, $\mu(s)$, the second damping function. (b) ——, $\mathrm{Im}[\Phi(s)]$, imaginary part of the radiation autocorrelation function. In the inset: ——, the first even pulse $p(s)$ of $\mathrm{Im}[\Phi(s)]$ represented for $s\geq 0$; — — —, $\mu(s)$, the second damping function. $h=12.6$, $x=375$, $V=-1.6\ 10^{14}\ \mathrm{s}^{-1}$. h is the number of perturbers in the interaction volume. x is the maximum value of the phase shift. V is the interaction potential.

$$\Phi_1(s)=p(s)*\sum_k \delta(s-k2\pi/V)\ . \quad (8)$$

This model for $\Phi(s)$ is illustrated in Fig. 2(a). The so-called "sampling function" $\sum_k \delta(s-k2\pi/V)$ is a pseudofunction with a Fourier transform (FT) proportional to

$$\sum_l \delta(\nu-lV/2\pi)\ ,$$

which is also a sampling function. Notice that the impulses, in the Fourier transform, are separated by $\nu=V/2\pi$.

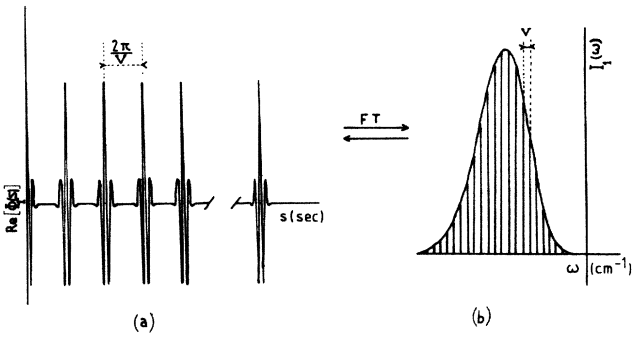

FIG. 2. (a) $\mathrm{Re}[\Phi_1(s)]$. (b) $I_1(\omega)$ (see text).

The Fourier transform of Eq. (8) is

$$I_1(\omega)=P(lV)\sum_l \delta(\omega-lV) . \tag{9}$$

$P(\omega)$ is the Fourier transform of $p(s)$. Rather than a convolution, we now have a direct product. Hence $I_1(\omega)$ is formed of infinitely narrow lines with amplitudes $P(lV)$. This spectrum is shown in Fig. 2(b).

The third remark concerning the autocorrelation function was the decrease of the maximum amplitudes of the different patterns $p(s-k2\pi/V)$ with k. This decrease is modeled perfectly by multiplying $\Phi(s)$ by a damping function $\gamma(s)$. An improved expression for the correlation is then

$$\Phi_2(s)=\Phi_1(s)\gamma(s)=p(s)*\sum\delta\left[s-k\frac{2\pi}{V}\right]\gamma(s) , \tag{10}$$

with a Fourier transform

$$I_2(\omega)=I_1(\omega)*\Gamma(\omega)=\left[\sum_l P(lV)\delta(\omega-lV)\right]*\Gamma(\omega) , \tag{11}$$

where $\Gamma(\omega)$ is the Fourier transform of $\gamma(s)$. The interpretation of this spectrum is straightforward; it is composed of Dirac shaped lines, each broadened in the same manner by convolution with $\Gamma(\omega)$. This is exactly what we obtain when taking the Fourier transform of the autocorrelation given in Fig. 1. The resulting profile $I_2(\omega)$ presents a series of broadened satellites separated by V. The envelope of the satellites is nothing but the Fourier transform of $\Phi(s)$ when it is truncated after the first pattern. This is illustrated in Fig. 3.

Notice that $p(s)$ has a very characteristic shape. It is a quasisinusoidal function weighted by a second damping function $\mu(s)$, as shown in Fig. 1(a). Then $p(s)$ is represented by

$$p(s)=\mu(s)\exp(i\omega_0 s) , \tag{12}$$

with FT,

$$P(\omega)=M(\omega+\omega_0) ,$$

if $\mu(s)=\mathrm{FT}[M(\omega)]$. The envelope, in our model, is then the FT of $\mu(s)$ simply shifted by ω_0. The envelope $E(\omega)$ of the satellites has the same shape as $P(\omega)$ but shifted by a quantity which is slightly different from ω_0 due to the loss of periodicity in the first pattern of $\Phi(s)$ and in the others as shown in Fig. 3.

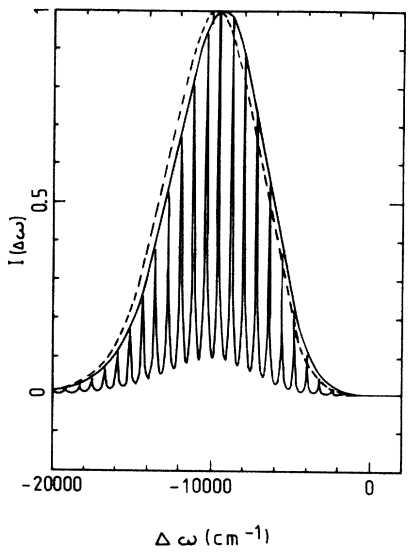

FIG. 3. $I(\Delta\omega)$: — — —, envelope $P(\Delta\omega)$; ——, shifted envelope $E(\Delta\omega)$.

This representation presents the great advantage that it permits a simple physical interpretation. Nevertheless, we have to notice that in Fig. 1 the different patterns in $\Phi(s)$ do not have exactly the same shape, since their halfwidths increase with increasing s. This may explain why the different satellites do not have exactly the same halfwidth (it increases with the order of the satellites). We shall now see that this approach suggested by the computed results is well corroborated by the analytical expression of the autocorrelation function.

IV. JUSTIFICATION OF THE MODEL BY THE MATHEMATICAL EXPRESSION OF THE AUTOCORRELATION FUNCTION

We need to consider only Eqs. (4) and (5) because we are concerned with large h for which the autocorrelation function becomes negligible when $u>1$. Because we study the limit of the strong interactions, we are concerned with large x, Eqs. (4) and (5) become

$$w(u)=\frac{3}{2}h\left[u+\left[u-\frac{u^3}{3}-\frac{2}{3}\right]\cos(xu)+\frac{2}{3}\right] , \tag{13}$$

$$d(u)=\frac{3}{2}h\left[\left[u-\frac{u^3}{3}-\frac{2}{3}\right]\sin(xu)\right] , \tag{14}$$

let

$$u=\frac{s}{\tau_{\max}} ,$$

$$\theta=\frac{3}{2\tau_{\max}} ,$$

and

$$xu = Vs \ .$$

In terms of these parameters, Eqs. (13) and (14) become

$$w(s) = h[1 + \theta s - (1 - \theta s + \tfrac{4}{27}\theta^3 s^3)\cos(Vs)] \ , \tag{15}$$

$$d(s) = -h(1 - \theta s + \tfrac{4}{27}\theta^3 s^3)\sin(Vs) \ . \tag{16}$$

These formulas show that large values of h cause a drastic damping as s increases. As a consequence, we need to consider only small s, and we define first-order expressions

$$w_1(s) = h[1 - \cos(Vs)] \tag{17}$$

and

$$d_1(s) = -h \sin(Vs) \ . \tag{18}$$

These expressions correspond to the function $p(s)$ introduced for the model in Sec. III as the pattern centered at $s=0$. Hence the spectrum $I_1(\omega)$ is composed of infinitely narrow lines. w_1 and d_1 are also the results obtained in the quasistatic limit $\bar{v} \to 0$. The corresponding spectrum is evidently composed of infinitely narrow lines because the duration of the wave trains and their autocorrelations continue to infinity (see Fig. 2). *Short-duration wave trains, on the contrary, lead to broad lines. It seems paradoxical to obtain the same results for two fundamentally different physical situations.*

This paradox arises from the fact that the autocorrelation function may not be written as Eqs. (17) and (18) for every s when h is large. Let us point out that in the quasistatic limit ($\bar{v} \to 0$) the correct FT needs considering, s going to infinity and hence taking all the patterns $p(s - k2\pi/V)$ into account. Therefore, this first-order limit is really meaningless for large density because the damping function has been neglected. This remark is fundamental because it shows clearly that the spectrum given by the *quasistatic limit is not equivalent to the high-density limit,* which is quite evident because they correspond to opposite physical situations.

However, if the autocorrelation function is restricted to the first pulse only, this implies that we need to consider only very small $s = s_{\max}$ such that $\theta s \ll 1$ [assuming that $\Phi(s) = 0$ for $s > s_{\max}$]. Since in this case we have

$$s \ll 2a/\bar{v} \ ,$$

the quasistatic theory is valid but only for the autocorrelation function. This is in agreement with Baranger[8] who discusses the validity of the static theory in terms of the autocorrelation function, giving as a condition the requirement that the autocorrelation function go to zero before a single collision is completed. A sufficient condition for this has been given by Royer[9] in the context of the Anderson-Talman theory,

$$n \gg 1/(4\pi R_0^3/3) \ ,$$

where R_0 is the radius of an "interaction volume" about the radiator which is equivalent for the square-well potential to $h \gg 1$.

But the correct FT is going to $s_{\max}$, not to infinity. We therefore need to know the damping function and to consider the second order. The correct expression for the limit of large h is

$$w_2(s) = h[1 + \theta s - (1 - \theta s)\cos(Vs)] \ , \tag{19}$$

$$d_2(s) = -h[(1 - \theta s)\sin(Vs)] \ . \tag{20}$$

Hence the autocorrelation function becomes

$$\Phi(s) = \exp[-(h\theta s)]\exp\{h[\cos(Vs) - 1]\}\exp[-(h\theta s)\cos(Vs)]\exp\{i[-h(1 - \theta s)\sin(Vs)]\} \ . \tag{21}$$

When $\cos(Vs) = 1$, this pseudoperiodic function presents maxima at $s = k2\pi/V$. Its value is then $\exp(-2h\theta s)$, which corresponds to the damping function $\gamma(s)$ of our representation. According to Eq. (10), the pattern function is

$$p(s) = \exp\{h[\cos(Vs) - 1]\} \times \exp\{i[-h(1 - \theta s)\sin(Vs)]\} \ . \tag{22}$$

If we restrict our study *to the first pulse only,* we can use instead

$$p(s) = \exp\{h[\cos(Vs) - 1]\}\exp\{-i[h \sin(Vs)]\} \ . \tag{23}$$

Notice in Eq. (22) that for subsequent pulses the approximation for $\theta s \ll 1$ given in Eq. (23) becomes poorer and poorer. These pulses are not identical. This proves that our representation was a little crude, and for decreasing h is quite poor because the correlation times of interest ($s_{\max}$) increase. We have shown here mathematically what has been noticed previously in the representation discussed in Sec. III. This model is excellent for the limiting case when h and x are large. We shall see that for decreasing h and x, the very peculiar shape of $\Phi(s)$, which presents well-separated patterns, deteriorates quite slowly. With this behavior in mind, this representation nevertheless allows an interpretation of these intermediate cases which present less characteristic patterns.

V. EVOLUTION OF THE AUTOCORRELATION FUNCTION WITH DECREASING h

A. Study of the computed profiles

In Figs. 1(a), 4, and 5 we have plotted the real parts of the autocorrelation function $\Phi(s)$ and in Figs. 3, 6, and 7 the corresponding profiles for $h = 12.56$, $h = 6.28$, and $h = 3.14$. In the first pattern $p(s)$, the number of oscillations and their peak-to-peak values decrease regularly with h. For these large values of h, $\Phi(s)$ still presents multiple pulses which lead to profiles with multiple satellites. The halfwidth of those satellites decreases predictably with h. For $h = 12.56$, the satellites are even a little

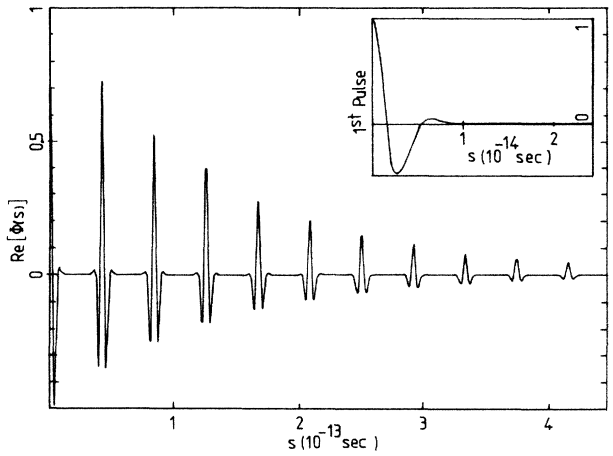

FIG. 4. Re[$\Phi(s)$]: $h=6.28$, $x=375$.

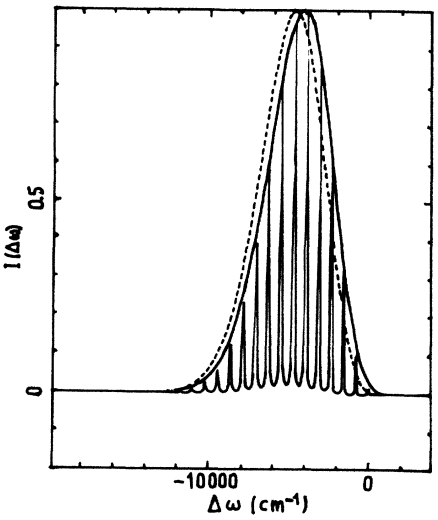

FIG. 6. $I(\Delta\omega)$: $h=6.28$, $x=375$. — — —, envelope $P(\Delta\omega)$; ——, shifted envelope $E(\Delta\omega)$.

blended and a continuum appears between them, but this phenomenon disappears for $h=3.14$.

The main line just appears in the profiles for $h=6.28$ and becomes more prominent for $h=3.14$. If we plot the Fourier transform of the first pulse, we notice that it is still the envelope of the satellites, but we must shift it by a variable quantity as discussed in Sec. III.

B. Study of the mathematical expression for the pulse

These properties may also be found with our representation. The pulse centered at $s=0$ is given by Eq. (22).

We first study the periodic damping function $\mu(s)=\exp\{-h[1-\cos(Vs)]\}$. The separation of two patterns in $\Phi(s)$ is the period $T=2\pi/V$, and $\mu(s)$ admits $T/2=\pi/V$ as an axis of symmetry. For large h, the damping function is bell shaped; it decreases steeply for small s $(0<s<T/4=\pi/2V)$, and is practically zero beyond $T/4$. In these situations, this strong periodic weighting implies that $\Phi(s)$ is composed of distinct patterns separated by gaps as shown in Fig. 8(a).

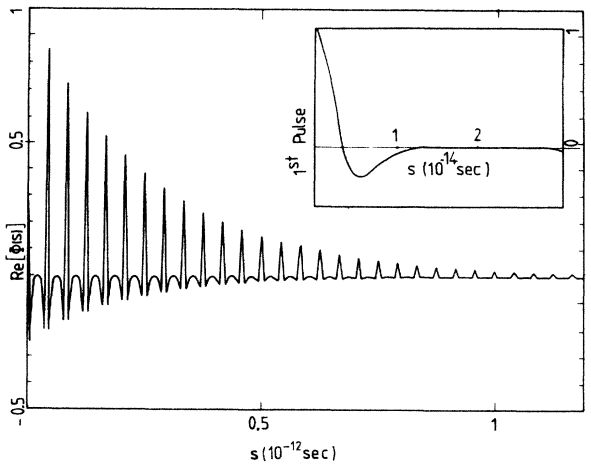

FIG. 5. Re[$\Phi(s)$]: $h=3.14$, $x=375$.

For smaller h, the damping becomes less and less severe. The value $\mu(\pi/V)=\exp(-2h)$ is not negligible compared to unity. The damping function also is no longer pulse shaped, but rather looks like a modulation function. $\Phi(s)$ now oscillates around a slowly decreasing function as shown in Fig. 8(c). Let us now study the real part of the oscillating portion of $p(s)$ given by

$$\cos[h\sin(Vs)] .$$

The zeros of this function are given by

$$\sin(Vs)=(2k+1)\pi/(2h) .$$

Because $|\sin(Vs)|<1$, there exists a $k_{\max}$ such that

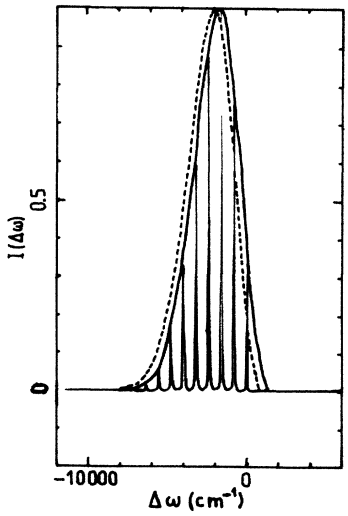

FIG. 7. $I(\Delta\omega)$: $h=3.14$, $x=375$. — — —, envelope $P(\Delta\omega)$; ——, shifted envelope $E(\Delta\omega)$.

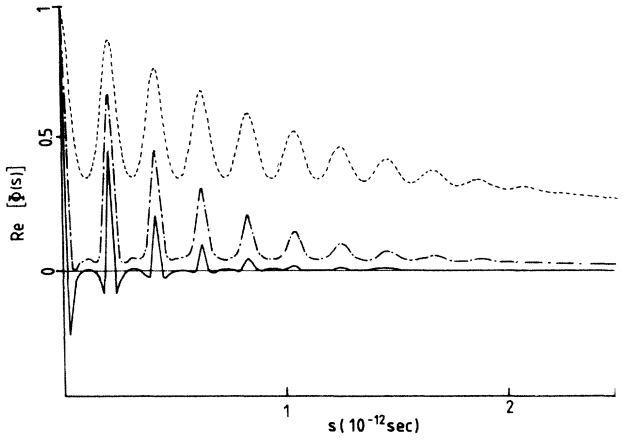

FIG. 8. Re[$\Phi(s)$]: (a) $h=3.14$, ——; (b) $h=1.57$, —·—·—·; (c) $h=0.5$, — — —. $x=75$.

$$k \leq k_{\max}=(h/\pi)-\tfrac{1}{2} .$$

Thus, for large h, many oscillations appear even if the damping $\mu(s)$ is quite severe. For example, when $h=12.56$, $\Phi(s)$ presents four zeros. With decreasing h, $k_{\max}$ decreases while the damping is still important. The number of oscillations decreases.

C. The particular case $h=\pi/2$

There is a very peculiar case when $h=\pi/2$, for which $k_{\max}=0$. $\Phi(s)$ then no longer has a negative region, and its only zero is for $s=\pi/2V$. Figure 8(b) shows $\Phi(s)$ in this case, and Fig. 9 is the corresponding profile. When h decreases down to 0.5, $\Phi(s)$ loses its distinctive shape with individual patterns separated by gaps. The gaps fill in completely and $\Phi(s)$ becomes a continuous oscillating function shown in Fig. 8(c) with the corresponding profiles in Fig. 10.

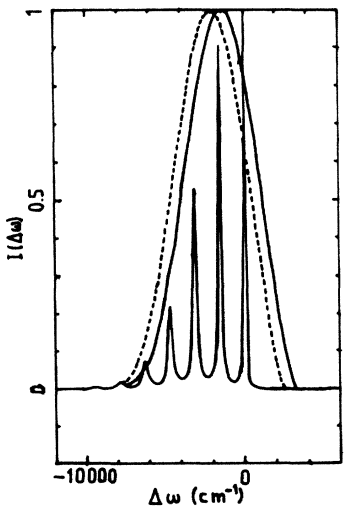

FIG. 9. $I(\Delta\omega)$: $h=1.57$, $x=75$; — — —, envelope $P(\Delta\omega)$; ——, shifted envelope $E(\Delta\omega)$.

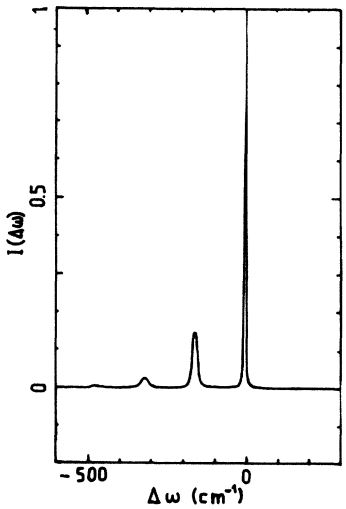

FIG. 10. $I(\Delta\omega)$: $h=0.5$, $x=75$.

D. Consequences for the shift

If we consider Eq. (22), we notice that the oscillating part of $p(s)$ is almost sinusoidal. The shift of the entire profile arises from this property. To evaluate the shift, we shall determine the absicssa s of the first zero of $p(s)$ from

$$\cos[h\sin(Vs_0)]=0, \quad h\sin(Vs_0)=\pi/2 ,$$

or

$$s_0=(1/V)\arcsin[\pi/(2h)] .$$

For large h,

$$s_0=\pi/(2hV) .$$

The period of the quasisinusoid is

$$T=4s_0=2\pi/(hV)$$

and the corresponding translation is

$$\delta=2\pi/T=hV .$$

This is exactly the shift d of the profile for $h=12$. This result validates the first-order development for small s in the limit for large h. For decreasing h the model worsens. Nevertheless, δ is a very good approximation of d for h as small as $\pi/2$.

This evaluation of $d=hV$ has been found previously in Sec. V of Ref. 2, but for the opposite limit of a weak interaction (small x).

For the particular case $h=\pi/2$,

$$\sin(Vs_0)=\pi/(2h)=1$$

or

$$s_0=\pi/(2V) .$$

This leads to $d=V$, which is the shift of the envelope, as illustrated in Figs. 9 and 11.

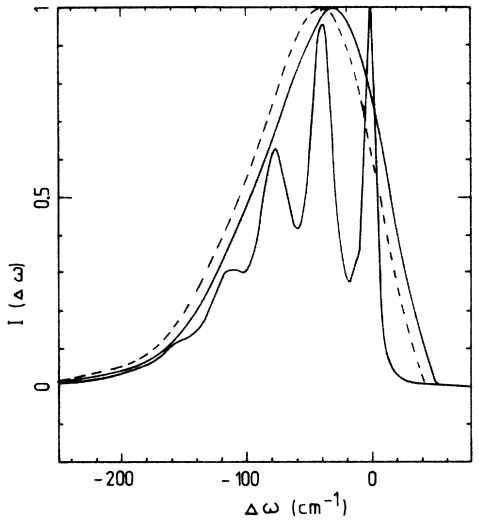

FIG. 11. $I(\Delta\omega)$: $h=1.57$, $x=18.75$; — — —, envelope $P(\Delta\omega)$; ——, shifted envelope $E(\Delta\omega)$.

The peculiar value of $h=\pi/2$ leads to discontinuities in the plots of the line parameters (width, shift, and asymmetry) versus density for satellites well separated from the line. These discontinuities have been discussed previously in Ref. 3 [Figs. 1(a), 4, and 5] and in Ref. 4

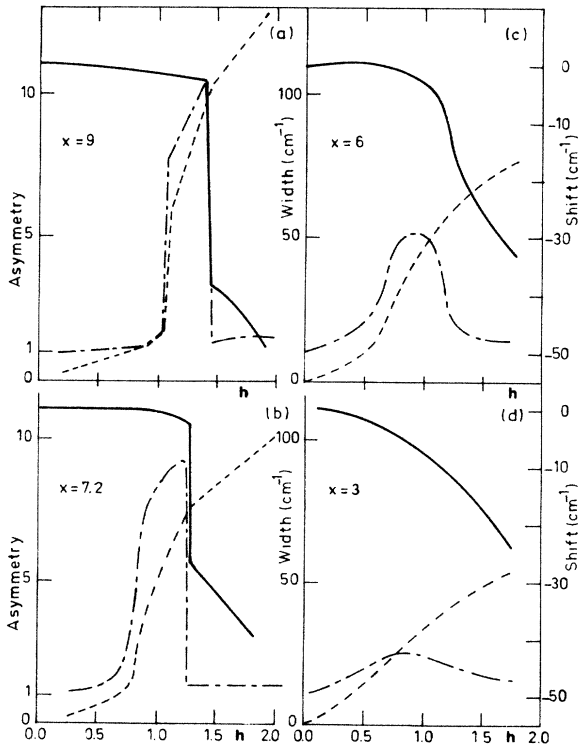

FIG. 12. Variation of width, shift, and asymmetry for different values of x. In each part the variations of w, d, and asym (width, shift, and asymmetry, respectively) are plotted vs h. The different scales for w, d, and asym are the same for the four x values. They are drawn with their respective units.

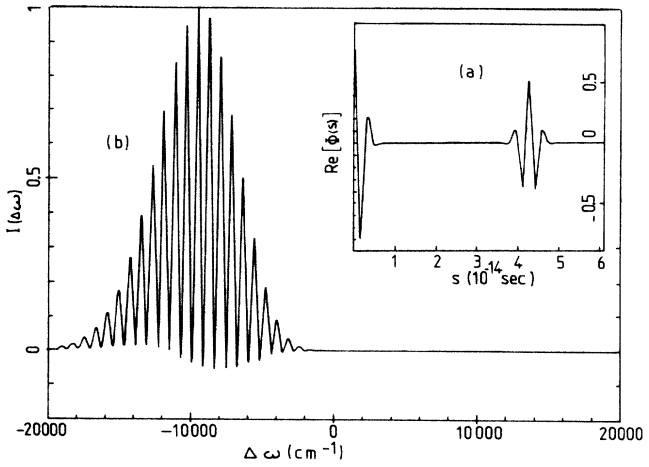

FIG. 13. (a) $\mathrm{Re}[\Phi(s)]$: $h=12$, $x=375$. (b) $I(\Delta\omega)$.

from which we have extracted Fig. 12. It is remarkable to find again this value here mathematically. In Sec. VI, we shall emphasize again the great importance of the parameter x and explain why the special case $x=6$ is the value for which discontinuities in line parameters shown in Fig. 12 first appear.

VI. PHYSICAL CONSEQUENCES OF THIS REPRESENTATION

We can see from Figs. 1(a), 4 and 5, that for a given x, the number of pulses which appear in the autocorrelation function depends on h due to the damping function. Let us calculate n_p, the maximum number of pulses. The pulses are separated by $s=2\pi/V$, and $\Phi(s)$ is a pseudo-periodical function for $s<\tau_{\max}$, where $\tau_{\max}=2a/\bar{v}$ is the maximum collision time. Therefore,

$$n_p=(\tau_{\max}/2\pi/\bar{v})+1$$

or

$$n_p=(x/2\pi)+1\ .$$

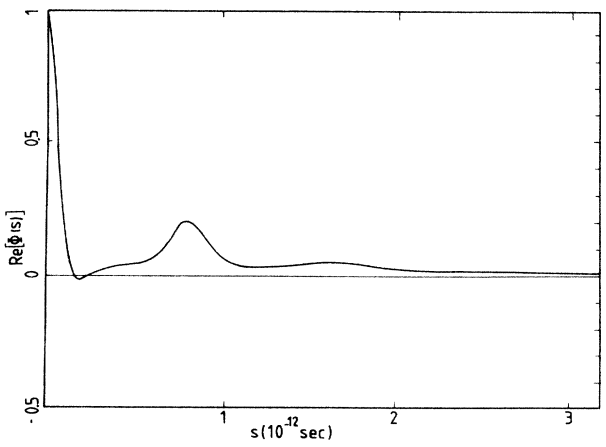

FIG. 14. $\mathrm{Re}[\Phi(s)]$: $h=1.57$, $x=18.75$.

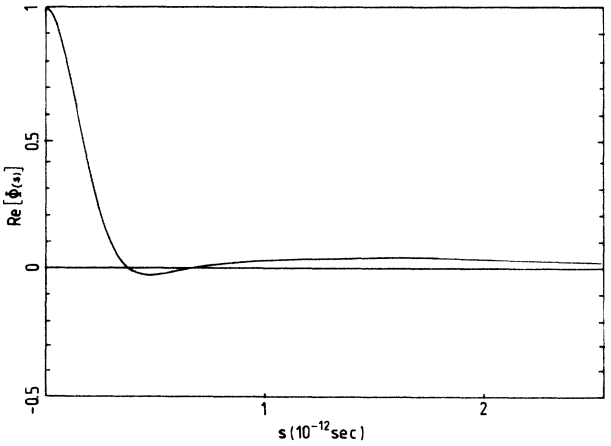

FIG. 15. Re[$\Phi(s)$]: $h=1.57, x=8.75$.

If $x<2\pi$, then $n_p=1$. In this case only one pulse exists and its Fourier transform leads to $P(\omega)$, what we have called the envelope in Eq. (12). Hence, it is clear that the condition $x>2\pi$ will be strictly necessary to get a profile which presents satellites.

We shall now prove that the presence of only two pulses in the autocorrelation is sufficient to get multiple satellites. In the case presented in Fig. 1 ($h=12, x=375$), we artificially truncate the autocorrelation just after the second pulse. The new autocorrelation function and the corresponding profile are shown in Fig. 13. We get multiple satellites separated by V just as in Fig. 3. This proves very clearly that $n_p=2$ is the necessary and sufficient condition for the appearance of multiple satellites.

These satellites will be more or less blended depending on the value of x. We shall now compare two cases with $x>2\pi$. In the first one, $x=18.75$, the pulse shape of $\Phi(s)$ is less striking than before. Nevertheless, three small bumps appear clearly in Fig. 14. They are sufficient to provide multiple, but now blended, satellites shown in Fig. 11.

For a smaller $x=8.75$, the autocorrelation is quite smooth, but a wide bump with a small amplitude still remains, as can be seen in Fig. 15. In Fig. 16, the first satellite appears clearly, but the second causes nothing but a shoulder, and the others are completely blended.

These important and new results are very gratifying to us. This is because, in our previous publications,[2,3] we have noticed that $x=2\pi$ was "a transition region between two characteristic families of line shapes." Now, in the present study, we are able to explain why $x=6$ was a special value.

This study emphasizes again that $x=V\tau_{\max}$ is the fundamental parameter. This is quite logical because it represents the maximum phase shift during the collision. This is similar to the statement of Weisskopf,[10,11] who said in 1932 that the collision is completed when the phase shift attains 1 rad. and defined in that way the so-called "Weisskopf radius." Our result establishes that the formation of a pseudomolecule, which provides multiple satellites demands a 2π phase shift.[12]

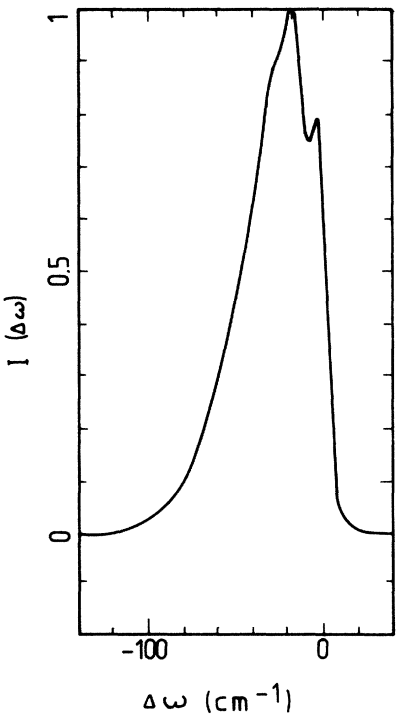

FIG. 16. $I(\Delta\omega)$: $h=1.57, x=8.75$.

VII. CONCLUSION

A very good practice of the spectral Fourier analysis has allowed us (1) to build a model well fitted to the autocorrelation of the radiation emitted during the collision in the case of high interactions and densities; this model being in good agreement with the mathematical formulas; (2) (perhaps most importantly) to follow and primarily to explain the variations of the autocorrelation (and hence of the spectra) when decreasing both interaction and density; (3) to explain (and not only describe) the discontinuities appearing in the plots of shift, width, and asymmetry versus density when decreasing the reduced variable $x=2aV/\bar{v}$; (4) at last to determine the condition $x\gg 2\pi$ necessary to obtain the collisional phase variation insuring the presence of multiple satellites.

ACKNOWLEDGMENTS

We gratefully acknowledge the Centre National de la Recherche Scientifique and the Centre Inter-Régional de Calcul Electronique, Orsay, France, for use of their facilities. One of us (A.C.) acknowledges financial support from Laboratoire de Physique Atomique et Moléculaire et d'Instrumentation en Astrophysique, which is Unité Associée au Centre National de la Recherche Scientifique No. 812. One of us (Y.G.B.) acknowledges financial support from Astronomie Infrarouge, which is Unité Associée au Centre National de la Recherche Scientifique No. 325.

[1]N. F. Allard, J. Phys. B **11**, 1383 (1978).
[2]N. F. Allard and Y. G. Biraud, J. Quant. Spectrosc. Radiat. Transfer **23**, 253 (1980).
[3]D. E. Gilbert, N. F. Allard, and S. Y. Ch'en, J. Quant. Spectrosc. Radiat. Transfer **23**, 201 (1980).
[4]N. F. Allard and Y. G. Biraud, J. Phys. (Paris) **44**, 935 (1983).
[5]S. Y. Ch'en, D. E. Gilbert, and D. K. L. Tan, Phys. Rev. **184**, 51 (1969).
[6]S. Y. Ch'en and R. O. Garrett, Phys. Rev. **144**, 59 (1966).
[7]P. W. Anderson and J. D. Talman, in Proceedings of the Conference on Broadening of Spectral Lines, Murray Hill, N.J., 1956 [Bell Telephone System Technical Publications Report No. 3117, 1956].
[8]M. Baranger, *Spectral Line Broadening in Plasmas in Atomic and Molecular Processes,* edited by D. R. Bates (Academic, New York, 1962), p. 493.
[9]A. Royer, Phys. Rev. A **22**, 1625 (1980).
[10]V. Weisskopf, Z. Phys. A **75**, 287 (1932).
[11]V. Weisskopf, Z. Phys. B **77**, 398 (1932).
[12]N. F. Allard, Y. G. Biraud, and A. Chevillot, C. R. Acad. Sci. (Paris) **304** (2), 14 (1987).